Early Jurassic magmatism on the Antarctic Peninsula and potential correlation with the Subcordilleran plutonic belt of Patagonia

Teal R. Riley [1]*, Michael J. Flowerdew[1,2], Robert J. Pankhurst[3], Mike L. Curtis[1,2], Ian L. Millar[3], C. Mark Fanning[4] & Martin J. Whitehouse[5]

[1]British Antarctic Survey, High Cross, Madingley Road, Cambridge, CB3 0ET, UK

[2]CASP, 181A Huntingdon Road, Cambridge, CB3 0DH, UK

[3]British Geological Survey, Keyworth, Nottingham, NG12 5GG, UK

[4]Research School of Earth Sciences, The Australian National University, Canberra ACT 0200, Australia

[5]Swedish Museum of Natural History, Box 50007, SE-104 05 Stockholm, Sweden

*Author for correspondence

e-mail: trr@bas.ac.uk

Tel. 44 (0) 1223 221423

Abstract: Early Jurassic silicic volcanic rocks of the Chon Aike Province (V1: 187 – 182 Ma) are recognised from many localities in the southern Antarctic Peninsula and northeast Patagonia and are essentially coeval with the extensive Karoo (182 Ma) and Ferrar (183 Ma) large igneous provinces of pre-breakup Gondwana. Until recently, plutonic rocks of this age were considered either rare or absent from the Antarctic Peninsula batholith, which was thought to have been mainly constructed during the Middle Jurassic and the mid-Cretaceous. New U-Pb zircon geochronology from the Antarctic Peninsula and recently published U-Pb ages from elsewhere on the Peninsula and Patagonia are used to demonstrate the more widespread nature of Early Jurassic plutonism. Eight samples are dated here from the central and southern Antarctic Peninsula. They are all moderately to strongly foliated granitoids (tonalite, granite, granodiorite) and locally represent the crystalline basement. They yield ages in the range 188 – 181 Ma, and overlap with published ages of 185 – 180 Ma from granitoids from elsewhere on the Antarctic Peninsula and from the Subcordilleran plutonic belt of Patagonia (185 – 181 Ma). Whilst Early Jurassic plutons of the Subcordilleran plutonic belt of Patagonia are directly related to subduction processes along the proto-Pacific margin of Gondwana, coeval volcanic rocks of the Chon Aike Province are interpreted to be directly associated with extension and plume activity during the initial stages of Gondwana break-up. This indicates that subduction was ongoing when Chon Aike Province volcanism started. The Early Jurassic plutonism on the Antarctic Peninsula is transitional between subduction-related and break-up related magamatism.

The plutonic rocks of the Antarctic Peninsula magmatic arc form one of the major batholiths of the proto-Pacific continental margin (Leat *et al.* 1995). The Antarctic Peninsula batholith is interpreted to extend for 1350 km and clear correlations can be established with plutonic rocks in the adjacent crustal blocks of West Antarctica and Patagonia (Fig. 1). An absence of reliable age data along large parts of the batholith mean that it is not possible to construct a chronology of its construction and any shifts in its magmatic axis during the Mesozoic. The Antarctic Peninsula batholith is dominated (>80%) by calc-alkaline tonalite-granodiorite-diorite compositions, with minor granite-quartz diorite-quartz monzodiorite, typical of a continental margin arc (e.g. Waight *et al.* 1998). The Antarctic Peninsula preserves a long-lived plutonic record, from the Ordovician (Riley *et al.* 2012) until at least 23 Ma (Jordan *et al.* 2014), although the batholith was largely constructed from the Middle Jurassic to mid-Cretaceous. Mesozoic magmatism along the proto-Pacific margin of Gondwana has widely been attributed to long-lived subduction (e.g. Leat *et al.* 1995), although episodic events, termed magmatic ‘flare-ups’ (Paterson & Ducea 2015; Riley *et al.* 2016), that contribute to the development of the batholith may have been related to other forcing factors (e.g. rifting, plate reconfiguration, mantle plume influence).

This paper presents new U-Pb geochronology from granite, tonalite and granodiorite from eight sites on the Antarctic Peninsula. The results are used in combination with recently published U-Pb zircon ages from isolated sites elsewhere on the Antarctic Peninsula and also from the Patagonian Andes to construct a more complete chronology of Mesozoic plutonism and to demonstrate how Early Jurassic volcanism and plutonism in the region are related.

Geological Setting

The Antarctic Peninsula was initially interpreted as an autochthonous continental arc of the Gondwana margin, which developed during Mesozoic subduction (Suarez 1976; Pankhurst 1982). Vaughan & Storey (2000) re-interpreted the evolution of the Antarctic Peninsula as a collage of paraautochthonous and allochthonous terranes accreted onto the Gondwana margin. The terrane hypothesis has recently been challenged by Burton-Johnson & Riley (2015) who favour a model involving in situ continental arc evolution.

The Mesozoic volcanic and sedimentary successions of the eastern Antarctic Peninsula all have a characteristic continental affinity (Riley and Leat, 1999) and in the northern Antarctic Peninsula they unconformably overlie Carboniferous – Triassic metasedimentary rocks of the Trinity Peninsula Group (Barbeau *et al.* 2010; Bradshaw *et al.* 2012). The Trinity Peninsula Group is estimated to have a thickness of at least 5 km, deposited as submarine fans along a continental margin (Hathway 2000); it overlaps with, and is likely to overlie Ordovician – Permian age crystalline basement (e.g. Millar *et al.* 2002; Bradshaw *et al.* 2012; Riley *et al.* 2012).

The Mesozoic sequences of the Antarctic Peninsula underwent low- to medium-grade metamorphism and deformation, potentially during the Palmer Land deformation event (107 – 103 Ma; Vaughan *et al.* 2002) or during an earlier Late Triassic – Early Jurassic Peninsula deformation event (Storey *et al.* 1987).

The Early – Middle Jurassic silicic volcanic rocks of the southern Antarctic Peninsula (Palmer Land) include the Brennecke and Mount Poster formations (Riley *et al.* 2001; Hunter *et al.* 2006), which form part of the wider first-stage event (V1) of the Chon Aike Province (Pankhurst *et al.* 2000). They are associated with minor basaltic successions (Riley *et al.* 2016) and extensive shallow marine sedimentary rocks of the Latady Group (Hunter & Cantrill 2006).

Granitoid plutonic rocks form the most widespread igneous outcrops on the Antarctic Peninsula, occurring as individual plutons, composite intrusions and an extensive batholith constructed during Mesozoic–Cenozoic time (Leat *et al.* 1995). The paucity of exposure and geochronological/geophysical data across large parts of the Antarctic Peninsula mean that it is not possible to know the full extent and connectivity of many exposed granitoid plutons.

Geochronology of the magmatic rocks of West Antarctica and Patagonia

Leat *et al.* (1995) collated and assessed all geochronological data for the Antarctic Peninsula available at the time (mostly Rb-Sr, K-Ar). They identified the most significant peak of magmatism as Early to mid-Cretaceous (particularly in Palmer Land). However, they also highlighted clear gaps in intrusive activity; one during the Early Jurassic was attributed to an episode of arc compression. The mid-Cretaceous peak in plutonic activity has been supported by more recent geochronology; Flowerdew *et al.* (2005), Leat *et al.* (2009) and Vaughan *et al.* (2012) have all demonstrated a major peak in pluton emplacement between 110 Ma and 105 Ma, as part of the extensive Lassiter Coast intrusive suite (Rowley *et al.* 1983). Mid-Cretaceous arc magmatism has also been recognised in the adjacent areas of Patagonia (Pankhurst *et al.* 1992; Hervé *et al.* 2007) and West Antarctica (Mukasa & Dalziel 2000; Riley *et al.* in press). Such extensive plutonism may be classified as a magmatic 'flare-up' (c.f. Paterson & Ducea 2015), where magma addition rates are up to 1000 times greater than 'normal' arc conditions. The exact triggers for changing arc tempos and higher magma production rates are uncertain, but 'flare-ups' are often associated with cycles of crustal thickening, followed by tectonic thinning. Subduction was probably ongoing during the mid-Cretaceous 'flare-up' and was potentially responsible for an increase in volatile fluxing into the mantle wedge. A similar analysis from the Sierra Nevada batholith of North America (Paterson & Ducea 2015) also identified a mid-Cretaceous magmatic peak with >70% of the magma added to the lower crust at 30 – 70km depth.

A Middle Jurassic magmatic 'flare-up' is also recognised, at approximately 170 Ma, and is largely represented on the Antarctic Peninsula and Patagonia as equivalent to the V2 (171 – 167 Ma) event of the silicic Chon Aike Volcanic Province (Pankhurst *et al.* 2000; Riley *et al.* 2010). In contrast to the Early Jurassic V1 volcanic event, the V2 episode is also accompanied by contemporaneous granites and granodiorites occurring in the same geographical area as the volcanic rocks (Pankhurst *et al.* 2000).

Early Jurassic volcanism in the Antarctic Peninsula and Patagonia is well recognised as belonging to the V1 episode (187 – 182 Ma) of the Chon Aike Province (Féraud *et al.* 1999; Pankhurst *et al.* 2000). Rhyolitic tuffs and ignimbrites of this episode dominate the thick (>2 km) volcanic successions and crop out in the southern Antarctic Peninsula (Brennecke and Mount Poster formations) and the North Patagonian Massif (Marifil Formation). The Marifil Formation (Malvicini & Llambías 1974) of northeast Patagonia consists of thick (75 – 100m), flat-lying, strongly welded, reddish ignimbrite units, interbedded with crystal and lapilli tuffs. The Brennecke Formation (Wever & Storey 1992) comprises silicic metavolcanic rocks that crop out at various localities in eastern Palmer Land (Fig. 2). The principal lithologies are massive rhyodacite lavas and welded pyroclastic rocks. The Mount Poster Formation of south-eastern Palmer Land (Fig. 2) comprises rhyodacitic, crystal-rich ignimbrite units, which reach a maximum thickness of almost 2 km and preserve evidence of an intracaldera setting (Riley *et al.* 2001).

Geochronological data for the Marifil Formation have been given by Rapela & Pankhurst (1995), Féraud *et al.* (1999) and Pankhurst *et al.* (2000), with ages of ca. 188 to 174 Ma. The majority of $^{40}Ar/^{39}Ar$ ages fall in the interval 187–182 Ma and a single U-Pb zircon age of 187 ± 3 Ma (BAS unpublished data), so it is possible the true age range could be narrower. The Mount Poster Formation and Brennecke Formation of the southern Antarctic Peninsula have been dated using U-Pb geochronology in the much narrower interval, 184 – 183 Ma; Pankhurst *et al.* (2000) dated two samples of the Brennecke Formation at 184 ± 2 Ma, whilst Hunter *et al.* (2006) dated several disparate exposures of the Mount Poster Formation, which range in age between 185 Ma and 178 Ma, and yielded an average age of 183.4 ± 1.4 Ma.

However, sub volcanic equivalents to the V1 volcanic event have never been recognised and Leat *et al.* (1995)’s analysis of the chronology of the Antarctic Peninsula batholith identified a near absence of Early Jurassic ages in the range 187 – 182 Ma. There is a similar picture in the North Patagonian Massif where there are also no identified local plutonic equivalents of the Marifil Formation.

It is also relevant here to mention the adjacent Ellsworth-Whitmore Mountains crustal block of West Antarctica (Fig. 1), which is a displaced terrane and was originally located adjacent to the southern Africa/Weddell Sea sector of the Gondwana margin (Storey *et al.* 1988a). The Ellsworth Mountains consist of a thick succession of Palaeozoic siliciclastic, volcanoclastic and volcanic rocks (Curtis & Lomas 1999), which are intruded by Jurassic-age, A-type granites (Lee *et al.* 2012). Rb-Sr whole rock ages (Millar & Pankhurst 1987) and U-Pb zircon ages (Lee *et al.* 2012) record Jurassic granitoid magmatism in the interval 181 – 164 Ma, indicating at least some overlap with the Early Jurassic plutonic rocks of the Antarctic Peninsula and Patagonia. The tectonic cause of the Ellsworth-Whitmore Mountains magmatism remains unclear as is its relation to volcanism on the Antarctic Peninsula. Storey *et al.* (1988b) favour an origin from Jurassic crustal melting and hybridization with mafic magmas, triggered by extension following a phase of compression.

Here we will investigate the case for a broader plutonic event at ~183 Ma using recently published geochronology, in combination with the new U-Pb zircon data presented in this paper.

Previous work

Several isolated outcrops of Early Jurassic granitoids from the Antarctic Peninsula and the Subcordillera plutonic belt of Patagonia have recently been dated and record U-Pb zircon ages in the interval, 187 – 181 Ma, coincident with the V1 volcanic event of the Chon Aike Province (Pankhurst *et al.* 2000). This recent geochronology will be reviewed here.

Patagonia

Rapela *et al.* (2005) reported U-Pb ages from granitoids from what they termed the Subcordilleran plutonic belt of northwest Patagonia, a linear, discontinuous suite of Early Jurassic plutonic rocks that extend, approximately north-south for >250 km to the west of the North Patagonian Massif (Fig. 3). The Subcordilleran plutonic belt lies slightly oblique to the present-day continental margin and is compositionally more felsic in the north and more mafic to the south. The Subcordilleran plutonic belt lies to the west of the North Patagonian Massif and Rapela *et al.* (2005) suggested a shift in the axis of plutonism from the Patagonian batholith to the west. Rapela *et al.* (2005) selected four granitoid samples for U-Pb analysis from the northern Subcordilleran plutonic belt, including a biotite-hornblende granodiorite and quartz monzodiorite. The four samples yielded ages of 181 ± 2, 181 ± 3, 185 ± 2 and 182 ± 2 Ma, all in the range 185 – 181 Ma. These are consistent with a $^{40}Ar/^{39}Ar$ (plagioclase) age for gabbroic rocks from the southern Subcordillera plutonic belt reported by Page and Page (1999) as 182.7 ± 1.0 Ma.

It is possible that the plutonic rocks of the Early Jurassic Subcordilleran plutonic belt continue further south, but are obscured by Cretaceous sedimentary rocks and Middle Jurassic rhyolitic ignimbrites of the V2 Chon Aike Formation. The Subcordilleran plutonic belt is distinct from the neighbouring Patagonian batholith (Fig. 3), where the oldest granitoids are Late Jurassic and the batholith is dominated by granitoids of Cretaceous to Neogene age (Hervé *et al.* 2007). Jurassic granitoids appear to be absent from the North Patagonian Massif (Fig. 3), i.e. there is no exposed sub volcanic equivalent to the Marifil Formation, although there are widespread Triassic (220 – 206 Ma) granites exposed, which are considered to share a common lower crustal source with the Marifil Formation volcanic rocks (Rapela & Pankhurst 1996). In the central part of the North Patagonian Massif, the Lonco-Trapial Formation is formed of mostly andesitic lavas and dykes, which have been dated at ~185 Ma ($^{40}Ar/^{39}Ar$ amphibole) by Zaffarana & Somoza (2012).. This age is coeval with the adjacent Marifil Formation, although the Lonco-Trapial Formation was interpreted by Zaffarana & Somoza (2012) as a distinct event. They concluded that the Lonco-Trapial Formation andesites and the granitoids of the Subcordilleran plutonic belt were both directly related to subduction along the proto-Pacific margin, whereas the V1 volcanism of the Marifil Formation may have been more closely linked to rifting and plume-related magmatism of the Karoo large igneous province (Riley *et al.* 2001).

Antarctic Peninsula

The geochronology of the Antarctic Peninsula batholith was reviewed by Leat *et al.* (1995) and indicated a clear gap in pluton emplacement during the Early Jurassic. However, Rb-Sr and K-Ar whole rock and mineral data can be affected by resetting following subsequent magmatic and metamorphic events. Therefore, the geochronology of the Antarctic Peninsula plutonism reviewed here will rely on more recently acquired U-Pb zircon geochronology to demonstrate the greater ubiquity of pluton emplacement at ~180 Ma.

Graham Land: Riley *et al.* (2012) dated crystalline metamorphic and magmatic rocks from eastern Graham Land that included three granitoids from the Eden Glacier and Avery Plateau (Fig. 2). The two samples from the Eden Glacier are a tonalite and quartz monzonite and both yielded ages of 185 ± 3 Ma, whilst a weakly deformed granodiorite from the Avery Plateau yielded an age of 184 ± 3 Ma. Pankhurst *et al.* (2000) also identified inheritance at ~184 Ma in the granitoids of eastern Graham Land. The Bildad Peak granite (Fig. 2), which was dated by Pankhurst *et al.* (2000) at 169 ± 2 Ma, had inherited grains at 186 and 185 Ma, whilst a granite from the Mapple Glacier (Fig. 2) was dated at 164 ± 2 Ma, with inheritance at 183 Ma. The presence of inherited Early Jurassic zircon grains in Middle Jurassic plutons emplaced at mid-crustal levels suggests that they are inherited grains are of plutonic origin and not from a volcanic source.

Palmer Land: Early Jurassic plutonism in the interval, 185 – 180 Ma age has been identified from several sites in Palmer Land, away from the primary areas of V1 volcanism (Brennecke and Mount Poster formations; Fig. 2). Leat *et al.* (2009) reported three Early Jurassic ages (U-Pb) from northwest Palmer Land; two weakly deformed granitic gneisses from Goettel Escarpment (Fig. 2) were dated at 180 Ma and 184 Ma (see Fig. 1b in Leat *et al.* 2009), coincident with Early Jurassic plutonism from elsewhere on the Antarctic Peninsula. Leat *et al.* (2009) also dated (183.0 ± 2.1 Ma) a felsic orthogneiss from Cape Berteaux in northwest Palmer Land (Fig. 2), although there is an element of uncertainty regarding the protolith. The sample is a medium grained, foliated felsic lithology, but a possible relict phenocryst texture led Leat *et al.* (2009) to interpret the protolith as volcanic. However, silicic volcanic rocks of ~183 Ma age are unknown outside eastern Palmer Land, so a plutonic origin to the protolith is preferred.

Flowerdew *et al.* (2006) examined the crustal source of granitic gneisses from eastern Palmer Land and identified several inherited core ages of ~180 Ma from a leucocratic gneiss at Mount Nordhill (Fig. 2), which is close to the sample site area of this study.

This study

A broad selection of granitoids from the southern Antarctic Peninsula were dated as part of a wider study investigating the tectonic evolution of the Antarctic Peninsula. Eight of the analysed samples recorded Early Jurassic ages and they form the basis of this study. Five samples are from eastern Palmer Land; sample R.2143.3 is a sheared granitoid from Engel Peaks (Fig. 2), N11.115.1 is a sheared tonalite from Mount Jackson (Fig. 2), R.7170 is a moderately sheared granodiorite from Mount Sullivan (Fig. 2), N10.395.2 is a moderately foliated granitoid from Eileson Peninsula (Fig. 2), whilst N10.470.1, also from the Eileson Peninsula is a sheared biotite granite. The three remaining samples analysed here are R.6308.1, a foliated granodiorite from the Batterbee Mountains (Fig. 2) and two samples from southernmost Graham Land; sample R.6157.1 is a granitic gneiss from Reluctant Island (Fig. 2, Loske *et al.* 1997) and sample BR.015.1 is a foliated granite from Roman Four Promontory (Hoskins 1963, Fig. 2).

Analytical procedures

U-Pb zircon geochronology was carried out using the Cameca IMS 1280 ion microprobe, housed at the NORDSIM isotope facility, Swedish Museum of Natural History (Stockholm) and the Sensitive High Resolution Ion Microprobe (SHRIMP) at the Australian National University, Canberra.

Zircons, separated by standard heavy liquid procedures were mounted in epoxy and polished to expose their interiors. They were imaged by optical microscopy and cathodo-luminesence (CL) prior to analysis. The CL images were used as guides for analysis targets because they reveal the internal structure of the grains. The analytical methods using the NORDSIM facility closely followed those detailed by Whitehouse & Kamber (2005). U/Pb ratio calibration was based on analysis of the Geostandard reference zircon 91500, which has a $^{206}Pb/^{238}U$ age of 1065.4 ± 0.6 Ma and U and Pb concentrations of 81 and 15 ppm respectively (Wiedenbeck *et al.* 1995). At the SHRIMP facility the analytical method followed that outlined by Williams (1998). Calibration was carried out using zircon standards mounted together with the samples (mostly AS-3; Paces & Miller 1993).

Common lead corrections (for NORDSIM data) were applied using a modern day average terrestrial common lead composition ($^{207}Pb/^{206}Pb$ = 0.83; Stacey & Kramers 1975) where significant ^{204}Pb counts were recorded. Age calculations were made using Isoplot v.3.1 (Ludwig 2003) and the calculation of concordia ages followed the procedure of Ludwig (1998). The results are summarised in Table 1. The uncertainty in the calculated ages is 2σ/95% confidence limits.

Results

Large broken zircon grains and squat prisms (>250 µm) were recovered from sample R.2143.3 (Engel Peaks). The majority of the grains exhibited diffuse growth zoning patterns under CL (Supplementary Fig. 1a). Evidence for zircon growth other than that during crystallisation of the granitoids was not detected. Seven analyses from 7 grains yield weighted mean of the $^{206}Pb/^{238}U$ ages of 188 ± 1 Ma and a MSWD of 1.9 (Fig. 4a), which is taken to date intrusion. Three analyses with large common Pb corrections were excluded from the age calculation as it is likely that these have also suffered some recent Pb loss.

Sample N11.115.1 (Mount Jackson) yielded prisms which typically range in length between 150 µm and 200 µm have aspect ratios of 3:1 and exhibit simple diffuse growth zoning. A thin <10 µm CL bright rim is ubiquitous (Supplementary Fig. 1b), and although this rim was not analysed, it probably grew during tonalite crystallisation along with the zircon with a diffuse zoning pattern. Inherited zircon cores are sometimes recognised using the CL images. Twenty analyses were carried out on 18 grains, 16 of which were located within zircon with a diffuse CL character. Excluding one analysis, which is interpreted to have suffered recent Pb loss, a weighted mean of the $^{206}Pb/^{238}U$ ages of 182 ± 1 Ma is calculated (Fig. 4b), and this age is interpreted to date the tonalite intrusion. Inherited grains yielded ages of c. 218 Ma, 465 Ma, 515 Ma and 969 Ma.

Zircons from the sheared granitoid sample N10.395.2 (Eileson Peninsula) are elongate prisms with 4:1 aspect ratios and are typically 200 – 250 µm long. Although the zircons are rather characterless under CL (Supplementary Fig. 1c), sector zoning is sometimes evident and it is likely that this zircon grew during granitoid intrusion. Inherited cores are not evident from the CL images. Ten analyses from 9 grains were carried out and excluding a single analysis from a possible inherited grain, and two analyses with large common Pb contents which have suffered recent Pb loss, a weighted average of the $^{206}Pb/^{238}U$ ages of 183 ± 1 Ma with an MSWD of 1.1 is calculated from the remaining grains (Fig. 4c), which is interpreted to date the intrusion of the granitoid.

Sample N10.470.1 (Eileson Peninsula) yielded prisms typically 200 µm long with 3:1 aspect ratios. Under CL, the zircons are generally featureless and non-luminescent (Supplementary Fig. 1d). Five analyses were carried out on 5 grains and excluding the 2 analyses with sufficiently high uranium contents that the calibration with 91500 standard may become inappropriate, the remaining 3 analyses yield a weighted average of the $^{206}Pb/^{238}U$ ages of 182 ± 2 Ma with an MSWD of 0.9 (Fig. 4d), which is taken to record the granite intrusion.

Zircons from sample BR.105.1 (Roman Four Promontory) are squat prisms with simple growth zoning patterns under CL. Textural evidence for multiple zircon inheritance or zircon growth subsequent to the growth zoned zircon is lacking. Seven analyses were carried out on 7 grains, five of which yielded a weighted average of the $^{206}Pb/^{238}U$ ages of 182 ± 2 Ma with an MSWD of 1.7 and is interpreted to date the intrusion. The remaining two analyses, which were also carried out on the same zircon growth zones are younger, likely suffered recent Pb loss and so have been excluded from the age calculation.

Sample R.7170.1 (Mount Sullivan) granodiorite contains zircons which are prismatic with 2:1 aspect ratio and are growth-zoned and inclusion-rich. Some grains apparently contain inherited cores, confirmed by a single core analysis which yielded a c. 238 Ma age. The remainder yield a weighted average of the $^{206}Pb/^{238}U$ ages of 183 ± 3 Ma with an MSWD of 1.1, which is taken to date intrusion.

Zircons from granodiorite gneiss R.6308.1 (Batterbee Mountains) are inclusion-rich prisms, which are occasionally large with long axes exceeding 500 µm. All grains exhibit a fine-scale CL growth zoning pattern and whilst evidence for inherited grains are evident, these are rare. Sixteen analyses from 15 grains which lack evidence for inheritance yield ages which range between 190 ± 5 Ma and 171 ± 8 Ma and a weighted mean of the $^{206}Pb/^{238}U$ ages of 181 ± 3 Ma (MSWD = 3.6). The high degree of scatter may have resulted from small degrees of Pb loss during subsequent tectonism. By excluding the youngest four analyses in the age calculation, any slight Pb loss might be circumnavigated and an age of 184 ± 2 Ma and a MSWD of 1.6 results. This age may therefore better estimate the age of the granite intrusion.

Sample R.6157.1 (Reluctant Island) contains c. 200 µm prismatic zircons with 3:1 aspect ratios. They display simple growth zoning patterns under CL and lack evidence for inherited grains. Of the ten analyses from ten different grains, one exhibits Pb loss and accompanying common Pb. Exclusion of this analysis a calculated weighted average of the $^{206}Pb/^{238}U$ ages of 184 ± 2 Ma results, which is interpreted to date crystallisation of the granitic gneiss protolith.

Discussion

New U-Pb geochronology presented here, in combination with recently published, high precision geochronology from elsewhere on the Antarctic Peninsula and Patagonia indicate that there is a distinctive plutonic event at ~183 Ma.

The well recognised major volcanic event at ~183 Ma that crops out in northern Patagonia and the southern Antarctic Peninsula forms the V1 event of the wider Chon Aike Province (Pankhurst *et al.* 2000). There is no known subvolcanic equivalent to the V1 volcanism in either of the regions where V1 volcanic rocks are widespread, although this could be a feature of the exposure level (Pankhurst *et al.* 2000). A feature of the entire Chon Aike Province is the migration of volcanism from the northeast of Patagonia towards the southwest of the region over ca. 25 Myr (Féraud *et al.* 1999; Pankhurst *et al.* 2000; Fig. 5); as pointed out by the latter authors, this pattern is also observed in the Gondwana pre-breakup position of the Antarctic Peninsula, with migration of volcanism from southern Palmer Land to northern Graham Land (Fig. 5). The migration of volcanism is consistent with the petrogenetic model of Riley *et al.* (2001) who demonstrated that the rhyolitic volcanic rocks were the result of lower crustal melting, associated with the development of highly fusible crust through volatile enrichment above a long-lived continental margin. A feature of the petrogenetic model is that large volume silicic volcanism dominates during the melting phase associated with extension, but once the fusible part of the crust is exhausted (typically <2 Myr) then the locus of magmatism migrates.

The geographical overlap of ~183 Ma plutonism with the V2 volcanism (171 – 167 Ma) in eastern Graham Land, shown as part of this study, is counter to the general model and migration of the Chon Aike Province, if indeed the ~183 Ma plutonism is the subvolcanic equivalent of the V1 volcanism.

However, there is no reported evidence of the ~183 Ma plutonic rocks in the same geographical area as the V1 volcanic fields.

Given the location of the identified ~183 Ma granitoid plutons across Patagonia and the Antarctic Peninsula (Figs. 2 and 3), the most likely petrogenetic scenario is that the phase of ~183 Ma plutonism was not directly related to the coeval volcanism of the V1 event. The granitoids of the Subcordilleran plutonic belt of northwest Patagonia have a linear (north-south) outcrop pattern (Fig. 3), sub parallel to the continental margin, to the west of the Patagonian batholith and were interpreted by Rapela *et al.* (2005) to represent a subduction-related magmatic arc along the proto-Pacific margin of Gondwana with the axis of magmatism shifting to the west from the Patagonian batholith. The timing of plutonism indicated that subduction was ongoing during the eruption of the V1 volcanism of the Marifil Formation on the North Patagonian Massif. Rapela *et al.* (2005) investigated the geochemistry and geochronology of the Subcordilleran plutonic belt granitoids (granodiorites and quartz monzodiorites) and compared them to the coeval volcanic rocks of the Chon Aike Province and also to the Triassic plutonic rocks from elsewhere in Patagonia. They concluded that the Early Jurassic plutonism of the Subcordilleran plutonic belt was not present elsewhere in Patagonia. The trace element geochemistry, however, is not particularly diagnostic and although typical of magmatic rocks in convergent continental margins, it is essentially akin to other Andean batholiths and also the volcanic rocks of Patagonia.

The outcrop pattern of Early Jurassic plutonic rocks of the Antarctic Peninsula do not show the same obvious linear outcrop pattern as the Subcordilleran plutonic belt of Patagonia. However, the dimensions of the Subcordilleran plutonic belt are approximately 350 km in length by 150 km width, which is not dissimilar to the extent of the Early Jurassic plutonism observed on the Antarctic Peninsula (Fig. 2).

Isotopic comparisons

Isotopic comparisons between different generations of felsic magmatism on the Antarctic Peninsula and Patagonia are also not particularly diagnostic (Fig. 6), as the source region characteristics are similar. Silicic volcanic rocks of the V1 and V2 events in Patagonia and the Antarctic Peninsula exhibit very similar initial ratios in $^{87}Sr/^{86}Sr$ (0.7065-0.7070) and εNd (-2 to -3; Riley *et al.* 2001), which are in turn very similar to the isotopic ratios from the Triassic granitoids of the North Patagonian Massif (Rapela & Pankhurst 1996). Much the same range in isotope values (Fig. 6) is also observed in the Middle Jurassic silicic volcanic rocks of the Thurston Island crustal block (Fig. 1) in West Antarctica (Riley *et al.* in press) and also the Cretaceous I-type granitoids of northeast Palmer Land (Wever *et al.* 1994). Local exceptions do occur, where upper crustal contamination has resulted in more enriched isotopic values (e.g. Mount Poster Formation; Riley *et al.* 2001).

Isotopic values from the ~184 Ma Subcordilleran plutonic belt are rather distinctive with $^{87}Sr/^{86}Sr_i$ values of 0.705 and εNd_i values of ~ -1 (Fig. 6); they therefore form a separate geochemical group to the Chon Aike volcanic rocks, and the plutonic rocks of the North Patagonian Massif and the Central Patagonian batholith (Rapela *et al.* 1992). A subset of the ~183 Ma plutonic rocks of the Antarctic Peninsula have published isotope geochemistry (Wever *et al.* 1994; Leat *et al.* 2009), including several of the plutons described as part of this study;in addition, two further granitoids (R.2143.3, R.7170.1) were analysed here (Table 2). Although there is some range in isotopic values from the ~183 Ma plutonic rocks, it is apparent that where upper crustal contamination isn't prevalent, then the granitoids have $^{87}Sr/^{86}Sr_i$ values of ~0.7055 – 0.7060 and εNd_i values of -1 to -5 (Fig. 6). These values overlap, in part, with those from the Subcordilleran plutonic belt, although there is also a clear trend towards the volcanic rocks of the V1 event, so a simple relationship to subduction isn't borne out by the isotope data alone.

Conclusions

1. New U-Pb geochronology data presented here from the Antarctic Peninsula, in combination with recently published high-precision geochronology from elsewhere on the Antarctic Peninsula and Patagonia indicate that there was a significant episode of granitoid emplacement in the interval 185 – 181 Ma, and not a hiatus as previously suggested (Leat *et al.* 1995).

2. The granitoid plutonism at ~183 Ma is coincident with the major episode of silicic ignimbrite volcanism, which crops out extensively in northeast Patagonia and the southern Antarctic Peninsula. This is the V1 event (187 – 182 Ma) of the wider Chon Aike Volcanic Province (Pankhurst *et al.* 2000).

3. There is no known sub-volcanic component to the V1 volcanic event in the geographical area of the exposed volcanism. However the V2 volcanic event (171 – 167 Ma) of the Antarctic Peninsula is characterised by an exposed subvolcanic equivalent (granitic plutonism) to the rhyolitic ignimbrites.

4. The ~183 Ma granitoids (mostly tonalite, quartz diorite, granodiorite) are considered to represent a distinct magmatic event from the contemporaneous V1 volcanism of the Chon Aike Province. The plutonic rocks of the Subcordilleran plutonic belt are associated with subduction-related magmatism along the proto-Pacific margin of Gondwana; implyingthat subduction was ongoing at the onset of Chon Aike Province volcanism. As suggested by Zaffarana & Samoza (2012), the silicic volcanic event could have been related the early stages of Gondwana breakup (Pankhurst *et al.*, 2000) and plume activity associated with the contemporaneous Karoo and Ferrar LIPs (183 Ma; Svensen *et al.* 2012; Burgess *et al.* 2015), whereas the plutonism was subduction-related.

5. The ~183 Ma granitoids of the Antarctic Peninsula are interpreted as potential correlatives of the 185 – 181 Ma granites of the Subcordilleran plutonic belt of north-western Patagonia. Both regions form relatively narrow belts, sub parallel to the proto-Pacific margin of Gondwana. The Antarctic Peninsula granitoids are isotopically distinct to the coeval V1 volcanic rocks (Brennecke and Mount

Poster formations; Riley et al. 2001), but are marginally more enriched compared to the granitoids of the Subcordilleran plutonic belt.

Acknowledgements and funding

This study is part of the British Antarctic Survey Polar Science for Planet Earth programme, funded by the Natural Environmental Research Council. Tom Watson, Ian Rudkin and the air operations staff at Rothera Base are thanked for their field support. The paper has benefited from the thoughtful reviews of Carlos Rapela and two anonymous referees. Kerstin Lindén and Lev Ilyinsky are thanked for their assistance at the NORDSIM facility. This is NORDSIM contribution number XXX.

References

Barbeau, D.L., Davis, J.T., Murray, K.E., Valencia, V., Gehrels, G.E., Zahid, K.M. & Gombosi, D.J. 2010. Detrital-zircon geochronology of the metasedimentary rocks of north-western Graham Land. *Antarctic Science*, **22**, 65–65.

Bradshaw, J.D., Vaughan, A.P.M., Millar, I.L. Flowerdew, M.J., Trouw, R.A.J., Fanning, C.M. & Whitehouse, M.J. 2012. Coarse Permo-Carboniferous conglomerates in the Trinity Peninsula Group at View Point, Antarctic Peninsula: Sedimentology, geochronology and isotope evidence for provenance and tectonic setting in Gondwana. *Geological Magazine*, **149**, 626–644.

Burgess, S.D, Bowring, S.A., Fleming, T.H. & Elliot, D.H. 2015. High-precision geochronology links the Ferrar large igneous province with early-Jurassic ocean anoxia and biotic crisis. *Earth and Planetary Science Letters,* **415**, 90-99.

Burton-Johnson, A. & Riley, T.R. 2015. Autochthonous vs. accreted terrane development of continental margins: A new in situ tectonic history of the Antarctic Peninsula. *Journal of the Geological Society, London*, **172**, 832-835.

Curtis, M.L. & Lomas, S.A. 1999. Late Cambrian stratigraphy of the Heritage Range, Ellsworth Mountains: implications for basin evolution. Antarctic Science, 11, 63-77.

Féraud, G., Alric, V., Fornari, M., Bertrand, H. & Haller, M. 1999. $^{40}Ar/^{39}Ar$ dating of the Jurassic volcanic province of Patagonia: migrating magmatism relating to Gondwana break-up and subduction. *Earth and Planetary Science Letters*, **172**, 83-96.

Flowerdew, M.J., Millar, I.L., Vaughan, A.P.M. & Pankhurst, R.J. 2005. Age and tectonic significance of the Lassiter Coast Intrusive Suite, Eastern Ellsworth Land, Antarctic Peninsula. *Antarctic Science*, **17**, 443-452.

Flowerdew, M.J., Millar, I.L., Vaughan, A.P.M., Horstwood, M.S.A. & Fanning, C.M. 2006. The source of granitic gneisses and migmatites in the Antarctic Peninsula: a combined U-Pb SHRIMP and laser ablation Hf isotope study of complex zircons. *Contributions to Mineralogy and Petrology*, **151**, 751–768.

Hathway, B. 2000. Continental rift to back-arc basin: Jurassic – Cretaceous stratigraphical and structural evolution of the Larsen Basin, Antarctic Peninsula. *Journal of the Geological Society, London*, **157**, 417-432.

Hervé, F., Pankhurst, R.J., Fanning, C.M., Calderón, M.A. & Yaxley, G.M. 2007. The South Patagonian batholith: 150 my of granite magmatism on a static plate margin. *Lithos*, 97, 373-394.

Hoskins, A.K., 1963. The basement complex of Neny Fjord, Graham Land. *British Antarctic Survey Scientific Report* No 43.

Hunter, M.A. & Cantrill, D.J. 2006. A new stratigraphy for the Latady Basin, Antarctic Peninsula: Part 2. Latady Group and basin evolution. *Geological Magazine*, **143**, 797-819.

Hunter, M.A., Riley, T.R., Cantrill, D.J., Flowerdew, M.J. & Millar, I.L. 2006. A new stratigraphy for the Latady Basin, Antarctic Peninsula: Part 1, Ellsworth Land Volcanic Group. *Geological Magazine*, **143**, 777-796.

Jordan, T.A., Neale, R.F., P.T. Leat, Vaughan, A.P.M., Flowerdew, M.J., Riley, T.R., Whitehouse, M.J. & Ferraccioli, F. 2014. Structure and evolution of Cenozoic arc magmatism on the Antarctic

Peninsula; a high resolution aeromagnetic perspective. *Geophysical Journal International*, **198**, 1758-1774.

Leat, P.T., Scarrow, J.H. & Millar, I.L. 1995. On the Antarctic Peninsula batholith. *Geological Magazine,* **132**, 399-412.

Leat, P.T., Flowerdew, M.J., Riley, T.R., Whitehouse, M.J., Scarrow, J.H. & Millar, I.L. 2009. Zircon U-Pb dating of Mesozoic volcanic and tectonic events in Northwest Palmer Land and Southeast Graham Land, Antarctica. *Antarctic Science*, **21**, 633-641.

Lee, H.M., Lee, J.I., Lee, M.J., Kim, J. & Choi, S.W. 2012. The A-type Pirrit Hills Granite, West Antarctica: an example of magmatism associated with the Mesozoic break-up of the Gondwana supercontinent. *Geosciences Journal*, **16**, 421-435.

Loske, W., Hervé, F., Miller, H. & Pankhurst, R.J. 1997. Rb-Sr and U-Pb studies of the pre-Andean and Andean magmatism in the Horseshoe Island area, Marguerite Bay (Antarctic Peninsula). *In*: Ricci, C.A. (ed*.) The Antarctic region: geological evolution and processes*. Siena, Terra Antartica Publication, 353-360.

Ludwig, K.R. 1998. On the treatment of concordant uranium-lead ages. *Geochimica et Cosmochimica Acta*, **62**, 665-676.

Ludwig, K.R. 2003. User manual for Isoplot 3.00: a geochronological toolkit for Microsoft Excel. *Berkeley Geochronology Centre Special Publications*, **4**, 1–70.

Malvicini, L. & Llambías, E.J. 1974.Geología y génesis del depósito de manganese Arroyo Verde, Provincia del Chubut. Actas del V Congreso Geológico Argentino, Villa Carlos Paz (Cordoba), Tomo II. Buenos Aries: Associación Geológica Argentina, 185-202.

Millar, I.L. & Pankhurst, R.J. 1987. Rb-Sr geochronology of the region between the Antarctic Peninsula and the Transantarctic Mountains: Haag Nunataks and Mesozoic granitoids. *In* Gondwana Six: Structure, Tectonics and Geophysics, G.D. McKenzie, ed., Geophysical Monograph, pp. 151-60, American Geophysical Union, Washington D.C.

Millar, I.L., Pankhurst, R.J. & Fanning, C.M. 2002. Basement chronology and the Antarctic Peninsula: recurrent magmatism and anatexis in the Palaeozoic Gondwana Margin. *Journal of the Geological Society, London* **159**, 145–158.

Mukasa, S.B. & Dalziel, I.W.D. 2000. Marie Byrd Land, West Antarctica: evolution of Gondwana's Pacific margin constrained by zircon U-Pb geochronology and feldspar common-Pb isotopic compositions. *Geological Society of America Bulletin*, 112, 611-627.

Paces, J.B. & Miller, J.D. 1993. Precise U-Pb ages of Duluth Complex and related mafic intrusions, northeastern Minnesota: Geochronological insights to physical, petrogenetic, paleomagnetic, and tectonomagmatic process associated with the 1.1 Ga Midcontinent Rift System. *Journal of Geophysical Research-Solid Earth*, **98B**, 13,997-14,013.

Page, S. & Page, R. 1999. Las diabasas y gabbros del Jurásico de la Precordillera del Chubut. *In* Caminos, R. (Ed.) Geologíca Argentina. Subsecretaría de Minería de la Nación, Servicio Geológico Minero Argentino, Instituto de Geología y Recursos Minerales, Anales, 29, 489-495.

Pankhurst, R.J., 1982. Rb-Sr geochronology of Graham Land, Antarctica. *Journal of the Geological Society, London*, 139, 701-711.

Pankhurst, R.J. & Rapela, C.W. 1995. Production of Jurassic rhyolite by anatexis of the lower crust of Patagonia. *Earth and Planetary Science Letters*, **134**, 23-26.

Pankhurst, R.J., Hervé, F., Rojas, L. & Cembrano, J. 1992. Magmatism and Tectonics in Continental Chiloé, Chile (42°-42°30'S.). *Tectonophysics*, **205**, 283-294.

Pankhurst, R.J., Riley, T.R., Fanning, C.M. & Kelley, S.P. 2000. Episodic silicic volcanism in Patagonia and the Antarctic Peninsula: chronology of magmatism associated with break-up of Gondwana. *Journal of Petrology*, **41**, 605-625.

Paterson, S.R. & Ducea, M.N. 2015. Arc Magmatic Tempos: Gathering the Evidence. *Elements*, **11**, 91– 98.

Rapela, C.W. & Pankhurst, R.J. 1995. Production of Jurassic rhyolite by anatexis in the lower crust of Patagonia. *Earth & Planetary Science Letters*, **134**, 23-36.

Rapela, C.W. & Pankhurst, R.J. 1996. Monzonite suites: the innermost Cordilleran plutonism of Patagonia. *Transactions of the Royal Society of Edinburgh, Earth Sciences*, **87**, 193-203.

Rapela, C.W., Pankhurst, R.J. & Harrison, S.M., 1992. Triassic 'Gondwana' granites of the Gastre district, North Patagonian Massif. *Transactions of the Royal Society of Edinburgh, Earth Sciences*, **83**, 291-304.

Rapela, C.W., Pankhurst, R.J., Fanning, C.M. & Herve, F., 2005. Pacific subduction coeval with the Karoo mantle plume: the Early Jurassic Subcordilleran belt of northwestern Patagonia. *In* Vaughan, A.P.M, Leat, P.T., Pankhurst, R.J. (Eds.), Terrane processes at the margins of Gondwana. Geological Society, London, Special Publications, 246, 217-239.

Riley, T.R. & Leat, P.T. 1999. Large volume silicic volcanism along the proto-Pacific margin of Gondwana: lithological and stratigraphcial investigations from the Antarctic Peninsula. *Geological Magazine,* **136**, 1-16.

Riley, T.R., Leat, P.T., Pankhurst, R.J. & Harris, C. 2001. Origins of large volume rhyolitic volcanism in the Antarctic Peninsula and Patagonia by crustal melting. *Journal of Petrology*, **42** 1043-1065.

Riley, T.R., Flowerdew, M.J., Hunter, M.A. & Whitehouse, M.J. 2010. Middle Jurassic rhyolite volcanism of eastern Graham Land, Antarctic Peninsula: age correlations and stratigraphic relationships. *Geological Magazine*, **147**, 581-595.

Riley, T.R., Flowerdew, M.J. & Whitehouse, M.J. 2012. U-Pb ion-microprobe zircon geochronology from the basement inliers of eastern Graham Land, Antarctic Peninsula. *Journal of the Geological Society, London,* **169**, 381–393.

Riley, T.R., Curtis, M.L., Flowerdew, M.J. & Whitehouse, M.J. 2016. Evolution of the Antarctic Peninsula lithosphere: evidence from Mesozoic mafic rocks. *Lithos*, **244**, 59-73.

Riley, T.R., Flowerdew, M.J., Pankhurst, R.J., Millar, I.L., Leat, P.T., Fanning, C.M. & Whitehouse, M.J. in press. A revised geochronology of Thurston Island, West Antarctica and correlations along the proto-Pacific margin of Gondwana. *Antarctic Science*.

Rowley, P.D., Kellogg, K.S., Vennum, W.R., Laudon, T.S., Thomson, J.W., O'Neil, J.M. & Lidke, D.J. 1983. Tectonic setting of the English Coast, eastern Ellsworth Land, Antarctica. *In* Thomson, M.R.A., Crame, J.A., Thomson, J.W. (Eds.) Geological evolution of Antarctica. Cambridge University Press, 467-473.

Stacey, J.S. & Kramers, J.D. 1975. Approximation of terrestrial lead evolution by a two-stage model. *Earth and Planetary Science Letters* **26**, 207-221.

Storey, B.C., Wever, H.E., Rowley, P.D. & Ford, A.B. 1987. Report on Antarctic fieldwork: the geology of the central Black Coast, eastern Palmer Land. *British Antarctic Survey Bulletin*, 145–155.

Storey, B.C., Dalziel, I.W.D., Garrett, S.W., Grunow, A.M., Pankhurst, R.J. & Vennum, W.R. 1988a. West Antarctica in Gondwanaland: crustal blocks, reconstruction and break-up processes. *Tectonophysics*, **155**, 381-390.

Storey, B.C., Hole, M.J., Pankhurst, R.J., Millar, I.L. & Vennum, W. 1988b. Middle Jurassic within-plate granites in West Antarctica and their bearing on the break-up of Gondwanaland. *Journal of the Geological Society, London*, **145**, 999–1007.

Suárez, M. 1976. Plate tectonic model for southern Antarctic Peninsula and its relation to southern Andes. *Geology*, **4**, 211–214.

Svensen, H., Corfu, F., Polteau, S., Hammer, O. & Planke, S. 2012. Rapid magma emplacement in the Karoo large igneous province. *Earth and Planetary Science Letters*, **325-326**, 1-9.

Vaughan, A.P.M. & Storey, B.C. 2000. The eastern Palmer Land shear zone: a new terrane accretion model for the Mesozoic development of the Antarctic Peninsula. *Journal of the Geological Society, London*, **157**, 1243–1256.

Vaughan, A.P.M., Pankhurst, R.J. & Fanning, C.M. 2002. A mid-Cretaceous age for the Palmer Land event, Antarctic Peninsula: implications for terrane accretion and Weddell Sea evolution. *Journal of the Geological Society, London*, 159, 113-116.

Vaughan, A.P.M., Leat, P.T., Dean, A.A. & Millar, I.L. 2012. Crustal thickening along the West Antarctic Gondwana margin during mid-Cretaceous deformation of the Triassic intra-oceanic Dyer Arc. *Lithos*, **142-143**, 130–147.

Waight, T.E., Weaver, S.D. & Muir, R.J. 1998. Mid-Cretaceous granitic magmatism during the transition from subduction to extension in southern New Zealand: a chemical and tectonic synthesis. *Lithos*, **45**, 469-482.

Whitehouse, M.J. & Kamber, B. 2005. Assigning dates to thin gneissic veins in high-grade metamorphic terranes: a cautionary tale from Akilia, southwest Greenland. *Journal of Petrology*, **46**, 291-318.

Wiedenbeck, M., Alle, P., Corfu, F., Griffin, W.L., Meirer, M., Oberli, F., Von Quadt, A., Roddick, J.C. & Spiegel, W. 1995. Three natural zircon standards for U-Th-Pb, Lu-Hf, trace element and REE analyses. *Geostandards Newsletter*, **19**, 1–23.

Wever, H.E. & Storey, B.C. 1992. Bimodal magmatism in northeast Palmer Land, Antarctic Peninsula: geochemical evidence for a Jurassic ensialic back-arc basin. *Tectonophysics*, **205**, 239–259.

Wever, H.E., Millar, I.L. & Pankhurst, R.J. 1994. Geochronology and radiogenic isotope geology of Mesozoic rocks from eastern Palmer Land, Antarctic Peninsula: crustal anatexis in arc-related granitoid gneiss. *Journal of South American Earth Sciences*, **7**, 69-83.

Williams, I.S. 1998. U-Th-Pb geochronology by ion microprobe. *In* McKibben, M.A. & Shanks, W.C. (eds.) *Applications of microanalytical techniques to understanding mineralizing processes* 7, 1-35, Reviews in Economic Geology.

Zaffarana, C.B. & Somoza, R. 2012. Palaeomagnetism and $^{40}Ar/^{39}Ar$ dating from Lower Jurassic rocks in Gastre, central Patagonia: further data to explore tectonomagmatic events associated with the break-up of Gondwana. *Journal of the Geological Society, London*, **169**, 371-379.

List of Figures

Fig. 1: Reconstruction of Gondwana at approximately 180 Ma showing the extent of the main granitoid batholiths of the proto-Pacific margin in West Antarctica and South America. TI: Thurston Island; MBL: Marie Byrd Land; AP: Antarctic Peninsula. Batholiths : PCB: Peruvian Coastal Batholith; PFB: Patagonian and Fuegian Batholiths; APB: Antarctic Peninsula Batholith; LCIS: Lassiter Coast Intrusive Suite.

Fig. 2: Map of the Antarctic Peninsula showing the extent of the V1 volcanism of the Mount Poster and Brennecke formations and the locations/ages of the Early Jurassic plutonic rocks. The extent of the mid-Cretaceous Lassiter Coast intrusive suite is also shown.

Fig. 3: Sketch map of southern South America (after Pankhurst *et al.* 2000) showing the extent of the V1 volcanism of the Marifil Formation, V2 volcanism of the Chon Aike Formation and the intermediate volcanism of the Lonco-Trapial Formation. The extent of the Andean batholith and the Subcordilleran plutonic belt are shown. NPM: North Patagonian Massif.

Fig. 4: Concordia diagrams for analysed zircons from the Antarctic Peninsula (a) R.2143.3 sheared granitoid from Engel Peaks; (b) N11.115.1 sheared tonalite from Mount Jackson; (c) N10.395.2 foliated granitoid from Eileson Peninsula; (d) N10.470.1 sheared biotite granite from Eileson Peninsiula; (e) R.7170 is a granodiorite from Mount Sullivan; (f) R.6308.1 granite from Batterbee Mountains; (g) R.6157.1 granitoid gneiss from Reluctant island; (h) BR.015.1 granite from Roman Four Promontory.

Fig. 5: Gondwana Pacific margin reconstruction at ~185 Ma showing the extent of the major large igneous provinces of the Karoo, Ferrar and the Chon Aike. The lines highlight the migration of silicic

volcanism from 185 Ma to 155 Ma towards the proto-Pacific margin (Pankhurst *et al.*, 2000). DML: Dronning Maud Land; MBL: Marie Byrd Land.

Fig. 6: $^{87}Sr/^{86}Sr_i$ vs. εNd_i for Early Jurassic magmatic rocks from the Antarctic Peninsula and Patagonia. Data sources: Marifil Formation (Pankhurst & Rapela 1995); Brennecke Formation (Riley *et al.* 2001); Mount Poster Formation (Riley *et al.* 2001); Subcordilleran plutonic belt (Rapela *et al.* 2005); Palmer Land plutonic rocks (Wever *et al.* 1994; Leat *et al.* 2009; this study; BAS unpublished data). NPM: North Patagonian Massif.

Supplementary Figure 1: Cathodoluminescence images of analysed zircon grains from sites on the Antarctic Peninsula. Circles indicate the position of analysis. (a) R.2143.3 Engel Peaks; (b) N11.115.1 Mount Jackson; (c) N10.395.2 Eileson Peninsula; (d) N10.470.1 Eileson Peninsula; (e) R.7170 Mount Sullivan; (f) R.6308.1 Batterbee Mountains; (g) R.6157.1 Reluctant island; (h) BR.015.1 Roman Four Promontory.

Supplemenatry text

Analytical methods: Sr and Nd isotope geochemistry

Samples were weighed into Savillex teflon beakers and spiked with mixed ^{149}Sm-^{150}Nd and single ^{84}Sr isotope tracers, prior to dissolution using HF-HNO_3-HCl. Ion exchange columns packed with Eichrom AG50x8 cation exchange resin were used to separate Sr and a bulk rare-earth element fraction. Sm and Nd were separated from the REE concentrate using EICHROM LN-SPEC columns. Sm fractions were loaded onto one side of an outgassed double Re filament assembly using dilute HCl, and analysed in a Thermo Scientific Triton mass spectrometer in static collection mode. Replicate analysis of the BCR-2 rock standard across the time of analysis gave a mean Sm concentration of 6.34

± 0.06 ppm (1-sigma, n=7). Nd fractions were also loaded onto one side of an outgassed double Re filament assembly using dilute HCl, and analysed in a Thermo Scientific Triton mass spectrometer in multi-dynamic mode. Nd data were normalised to $^{146}Nd/^{144}Nd$ = 0.7219. Across the time of analysis, 19 analyses of the JND-i standard gave a value of 0.512102 ± 0.000005 (10.4 ppm, 1-sigma). All other standard and sample data is quoted relative to a value of 0.512115 for this standard. Seven analyses of La Jolla gave 0.511864 ± 0.000006 (11.5 ppm, 1-sigma). Replicate analysis of the BCR-2 rock standard gave a mean Nd concentration of 28.1 ± 0.3 ppm and $^{143}Nd/^{144}Nd$ = 0.512638 ± 0.000006 (11.9 ppm, 1-sigma, n=12). Sr fractions were loaded onto outgassed single Re filaments using a TaO activator solution, and analysed in a Thermo-Electron Triton mass spectrometer in multi-dynamic mode. Data were normalised to $^{86}Sr/^{88}Sr$ = 0.1194. Across the time of analysis, 143 analyses of the NBS987 standard gave a value of 0.710250 ± 0.000006 (9 ppm, 1-sigma). Replicate analyses of the BCR-2 rock standard run with the samples gave a mean Sr concentration of 340.6 ± 5.1 ppm, and $^{87}Sr/^{86}Sr$ = 0.705041 ± 0.00023 (33 ppm, 1-sigma, n=15). The calculated Rb/Sr (weight) ratio for BCR-2 is 0.1379 ± 0.0013 (1-sigma).

Riley et al.
Fig. 1

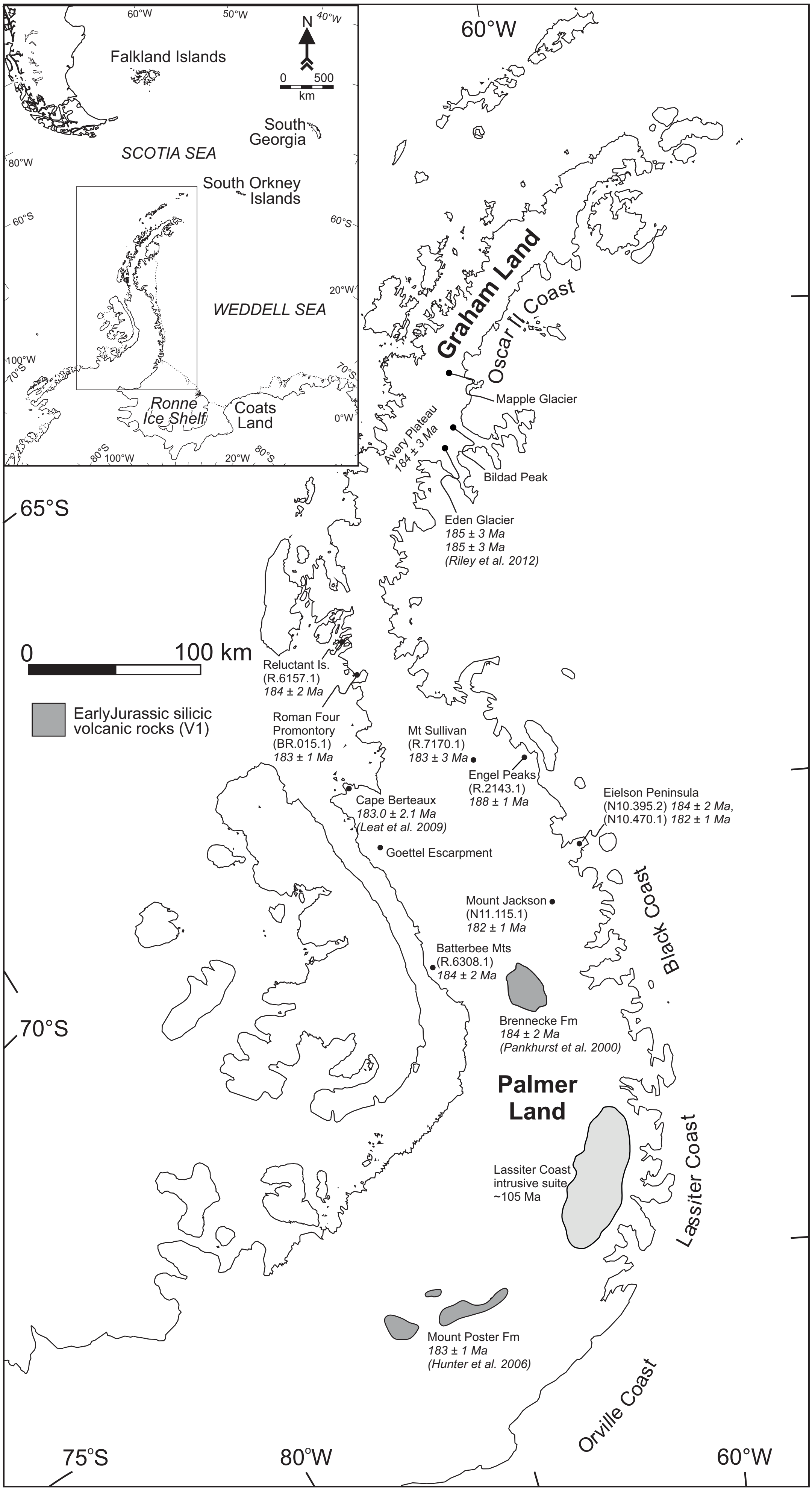

Riley et al.
Fig. 2

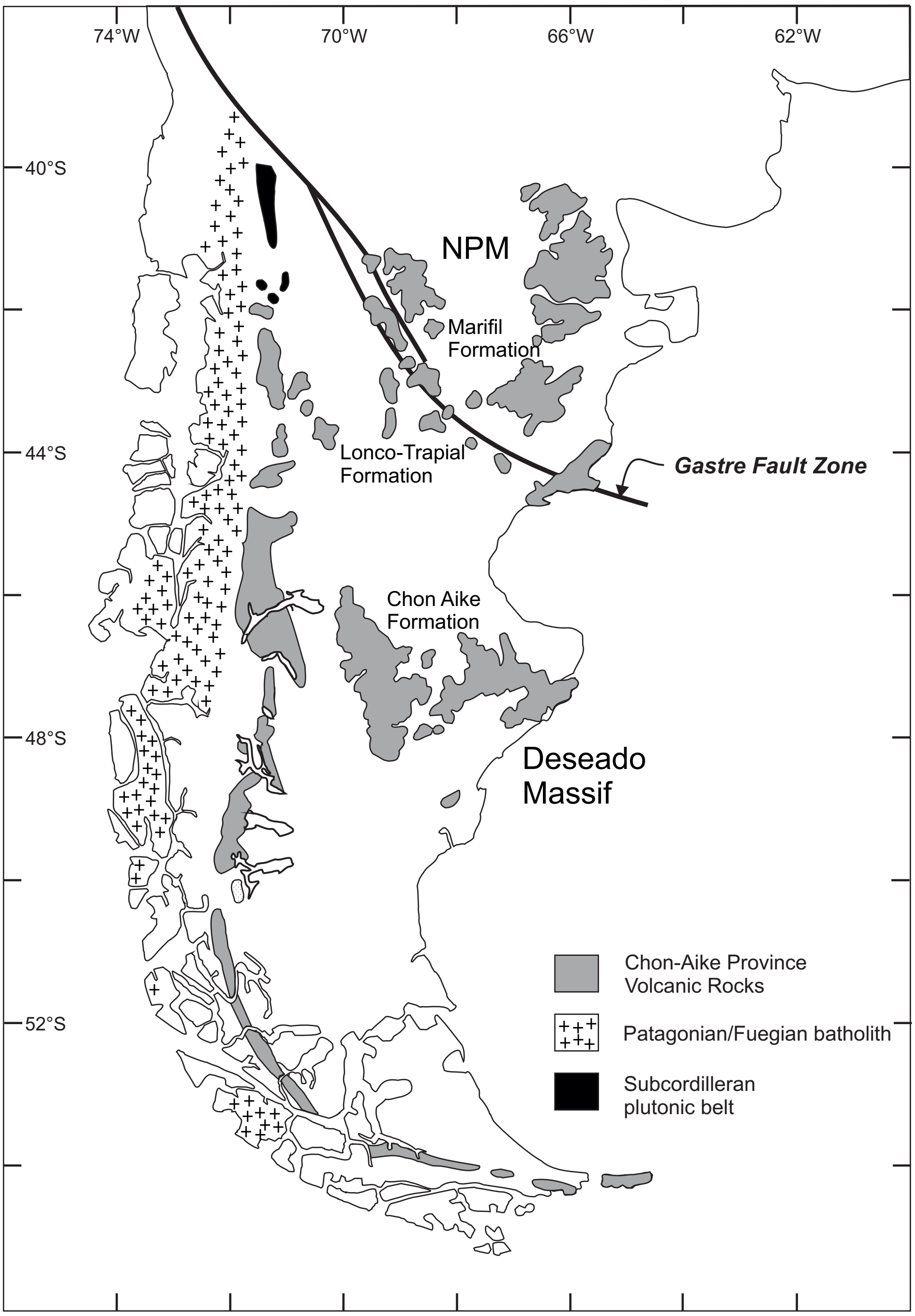

Riley et al.
Fig. 3

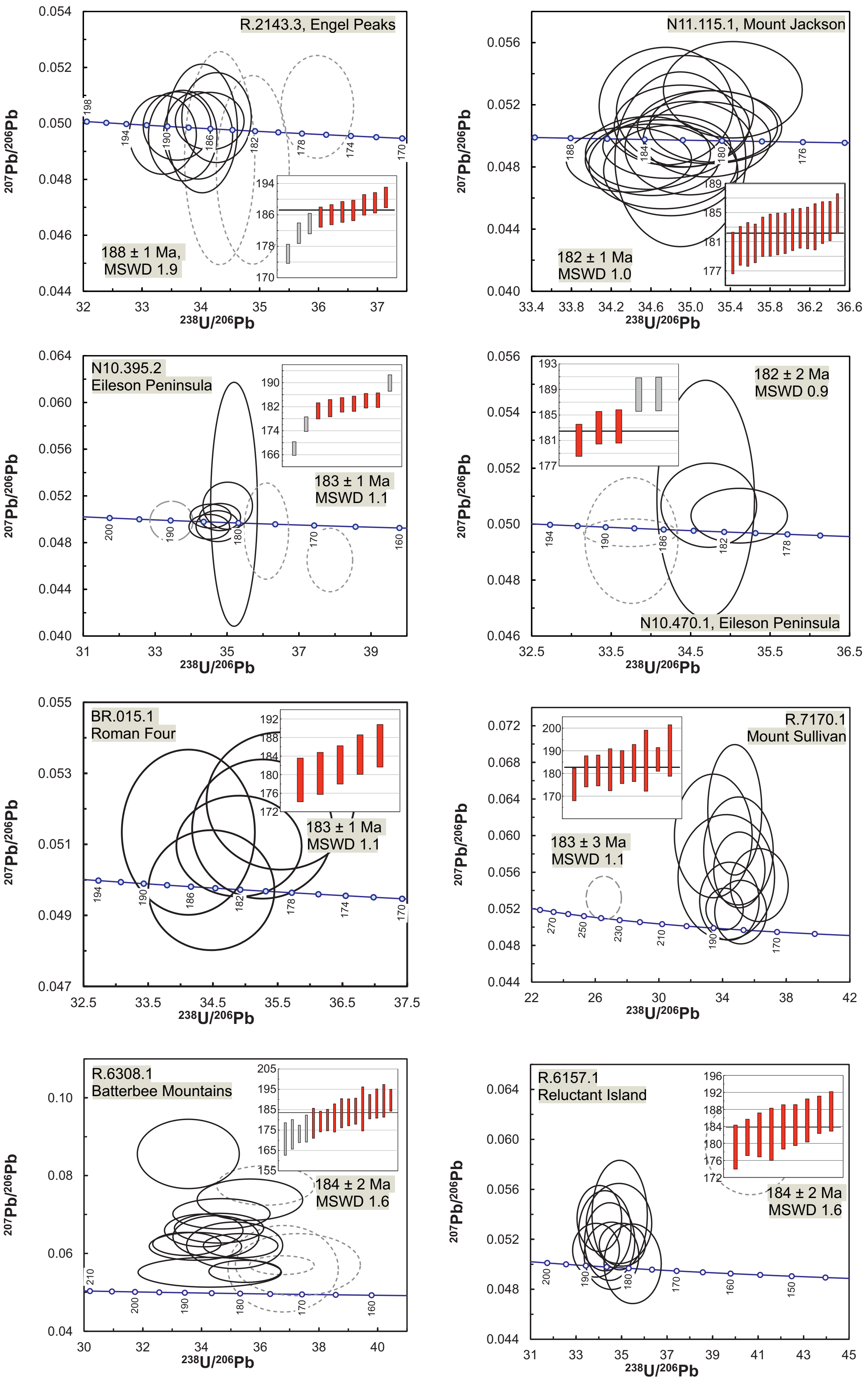

Riley et al.
Fig. 4

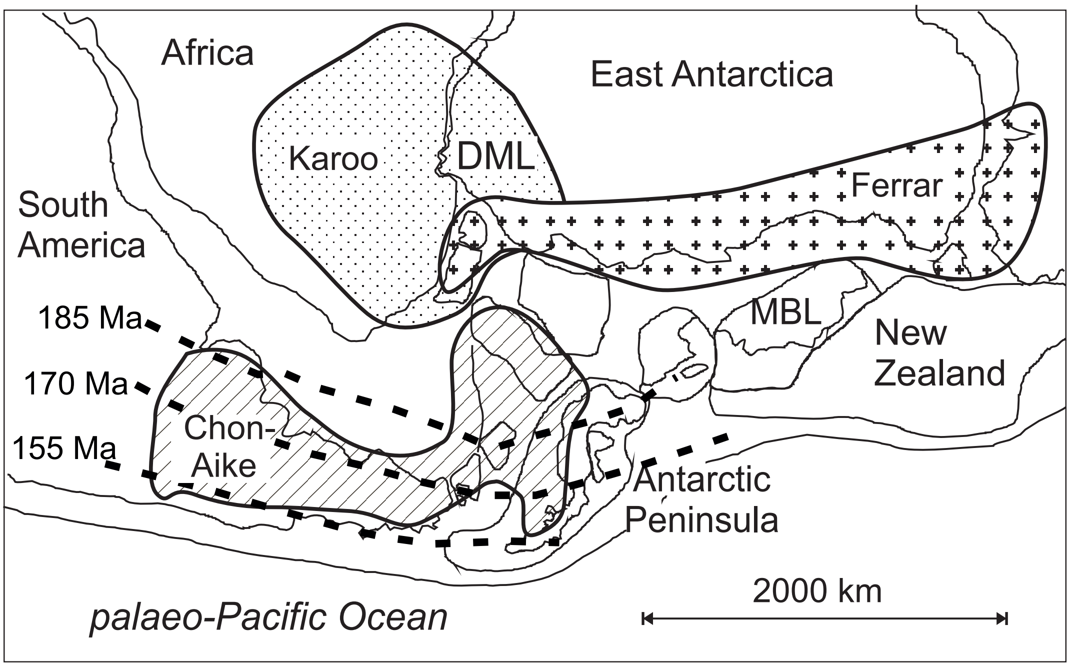

Riley et al.
Fig. 5

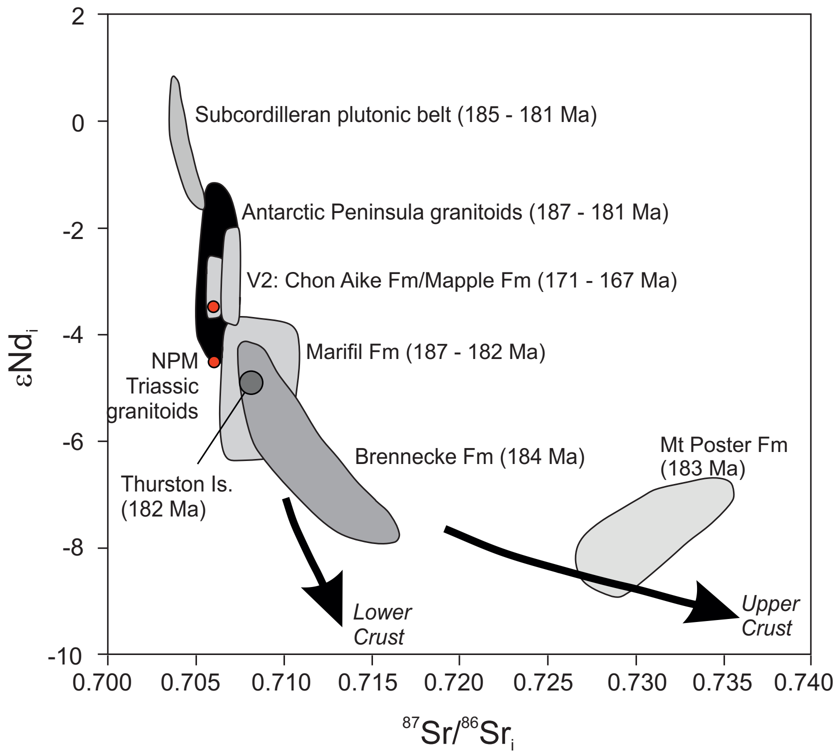

Riley et al.
Fig. 6

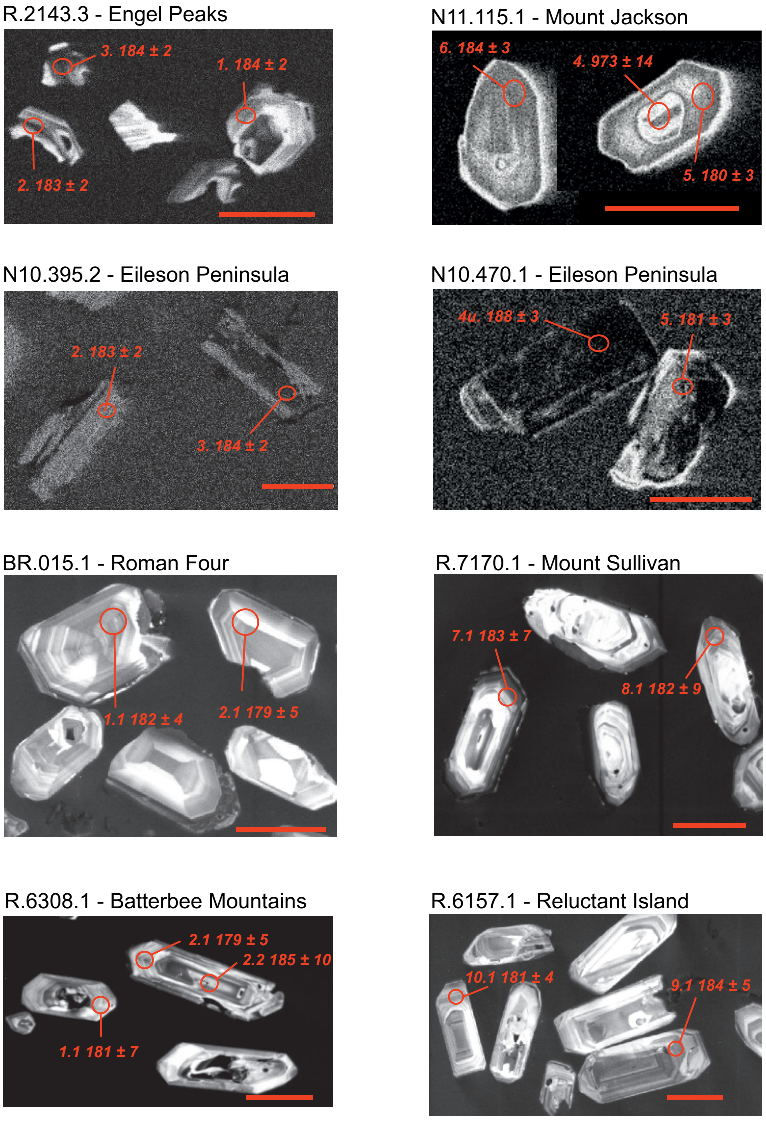

Riley et al.
Supplementary Fig. 1

Table 1: Zircon U-Pb ion-microprobe geochronology

Spot[1]	U (ppm)	Th (ppm)	Pb (ppm)	Th/U	f^{206} (%)[2]	$^{238}U/^{206}Pb$	±σ (%)	$^{207}Pb/^{206}Pb$	±σ (%)	$^{207}Pb/^{206}Pb$ age (Ma)	±σ	$^{206}Pb/^{238}U$ age (Ma)	±σ
NORDSIM data													
N11.115.1. Mount Jackson sheared tonalite													
9x	135	65	4	0.48	0.28	38.029	0.82	0.04819	2.62	108.4	60.7	167.3	1.3
5	128	45	4	0.35	0.00	35.425	0.81	0.05296	2.39	327.3	53.4	179.5	1.4
16	166	95	6	0.58	0.27	35.230	0.75	0.05061	1.86	222.9	42.3	180.4	1.3
18	166	68	6	0.41	0.29	35.191	0.84	0.05056	1.90	220.8	43.3	180.6	1.5
19	145	64	5	0.44	0.14	35.164	0.74	0.04977	1.98	184.3	45.5	180.8	1.3
17	160	77	6	0.48	0.23	34.987	0.76	0.04921	2.50	158.1	57.5	181.7	1.4
2	103	38	3	0.37	0.26	34.943	0.81	0.05159	2.83	267.1	63.8	181.9	1.4
11	171	97	6	0.56	0.31	34.911	0.80	0.05062	2.13	223.8	50.1	182.1	1.4
21	135	62	5	0.46	[1.37]	34.896	0.77	0.04849	4.74	123.3	107.9	182.1	1.4
1	166	78	6	0.47	0.08	34.800	0.79	0.04777	2.49	87.7	57.9	182.6	1.4
15	198	103	7	0.52	0.25	34.760	0.76	0.04931	1.69	162.7	40.1	182.8	1.4
7	107	44	4	0.41	0.19	34.752	0.79	0.05191	2.98	281.6	66.7	182.9	1.4
3	126	51	4	0.40	0.11	34.721	0.88	0.04817	2.43	107.6	56.4	183.0	1.6
6	197	90	7	0.46	0.17	34.611	0.79	0.04846	1.94	121.7	46.3	183.6	1.4
20	202	112	7	0.55	0.09	34.571	0.74	0.04890	1.96	143.0	45.3	183.8	1.3
14	180	104	6	0.58	0.12	34.378	0.75	0.04847	1.76	122.3	41.0	184.8	1.4
12i	150	75	7	0.50	[0.91]	28.341	1.67	0.07021	7.04	934.6	138.2	223.5	3.7
8i	135	32	11	0.24	0.08	13.331	2.42	0.05785	3.07	523.9	66.0	466.3	10.9
13i	160	71	16	0.45	0.13	12.013	0.85	0.05772	1.21	519.0	26.4	515.5	4.2
4i	199	114	41	0.57	0.05	6.137	0.77	0.07507	0.68	1070.5	13.6	973.2	7.0
R.2143.3. Engel Peaks, sheared granitoid													
6x	307	228	11	0.74	[0.36]	35.980	0.70	0.05059	1.48	-79.9	48.7	176.1	1.2
8x	170	135	6	0.80	[0.48]	34.882	0.73	0.04834	2.85	157.3	79.9	181.3	1.3
10x	62	31	2	0.51	[0.74]	34.320	0.71	0.04876	3.19	-175.7	140.9	183.8	1.3
7	380	306	14	0.81	0.26	34.266	0.70	0.05021	1.31	204.6	38.9	185.4	1.3
9	993	973	40	0.98	0.11	34.150	0.70	0.05009	0.84	199.0	21.6	186.1	1.3
4	192	116	7	0.60	0.12	34.020	0.72	0.04982	1.89	186.5	43.3	186.8	1.3
2	636	541	25	0.85	0.04	33.952	0.71	0.04957	1.29	174.9	29.7	187.1	1.3
1	380	332	15	0.87	0.22	33.691	0.71	0.04956	1.33	174.6	39.5	188.6	1.3
5	760	753	31	0.99	0.14	33.595	0.70	0.04991	1.00	190.7	26.3	189.1	1.3
3	499	514	20	1.03	0.17	33.352	0.70	0.04959	1.16	176.0	32.6	190.4	1.3
N10.395.2. Eileson Peninsula, sheared granitoid													
4x	742	358	23	0.48	[1.51]	37.858	0.68	0.04651	2.39	24.3	56.3	168.1	1.1
10x	5133	3822	179	0.74	[0.93]	36.092	0.70	0.04899	3.44	147.1	78.6	176.2	1.2
9	3371	2399	123	0.71	[1.46]	35.194	0.75	0.05128	8.32	253.6	180.9	180.6	1.3
5	144	60	5	0.42	0.18	35.018	0.80	0.05116	1.61	247.9	36.7	181.5	1.4
2	505	338	18	0.67	0.16	34.805	0.67	0.05019	0.95	203.8	26.0	182.6	1.2
6	421	139	14	0.33	0.05	34.734	0.70	0.04941	1.09	167.4	25.3	183.0	1.3
1	850	731	33	0.86	0.20	34.541	0.67	0.05027	0.83	207.6	25.0	184.0	1.2
3	1555	1601	62	1.03	[0.35]	34.505	0.67	0.04935	0.88	164.6	20.4	184.2	1.2
8i	5132	3102	194	0.60	[1.49]	33.453	0.73	0.04983	1.41	187.0	32.4	189.9	1.4
N10.470.1. Eileson Peninsula, sheared biotite granite													
5	600	138	19	0.23	0.07	35.112	0.71	0.05030	0.79	209.0	19.9	181.0	1.3
6	487	280	17	0.57	0.37	34.729	0.71	0.05068	1.21	226.1	44.5	183.0	1.3
2	580	442	22	0.76	[3.04]	34.689	0.72	0.05090	3.41	236.3	76.8	183.2	1.3
4u	1120	1127	45	1.01	[0.62]	33.756	0.71	0.04942	1.86	167.6	42.9	188.2	1.3
1u	2534	2972	107	1.17	0.04	33.741	0.71	0.04969	0.41	180.7	9.9	188.3	1.3
SHRIMP data													
BR.015.1. Roman Four granite													
5.1	659	245	21	0.4	0.17	39.842	1.23	0.0510	1.82	242.2	4.4	159.8	2.0
4.1	2522	1165	85	0.5	6.87	38.233	2.78	0.1043	7.27	1702.4	123.7	166.4	4.6
2.1	552	292	21	0.5	0.32	35.544	1.31	0.0522	1.51	295.1	4.5	178.9	2.4
3.1	532	281	20	0.5	0.22	35.263	1.26	0.0514	1.56	260.1	4.0	180.3	2.3
1.1	1486	1061	60	0.7	0.16	34.903	1.13	0.0510	1.14	238.6	2.7	182.1	2.1
6.1	966	578	38	0.6	0.00	34.476	1.15	0.0497	1.39	181.5	2.5	184.3	2.1
7.1	885	505	35	0.6	0.21	34.120	1.23	0.0513	1.85	256.1	4.7	186.2	2.3
R.6157.1. Reluctant Island gneiss													
8.1x	198	63	6	0.32	1.31	40.660	1.98	0.0595	2.69	585.1	15.7	156.6	3.1
1.1	417	186	15	0.45	0.04	35.487	1.45	0.0500	2.60	196.9	5.1	179.1	2.6
10.1	743	608	31	0.82	0.23	35.035	1.18	0.0516	1.36	266.4	3.6	181.4	2.1
4.1	250	118	9	0.47	0.53	34.920	1.42	0.0539	3.32	368.5	12.2	182.0	2.6
6.1	244	73	9	0.30	0.44	34.890	1.68	0.0533	2.46	340.3	8.4	182.2	3.1
9.1	512	401	21	0.78	0.12	34.559	1.42	0.0507	2.17	226.3	4.9	183.9	2.6
5.1	525	202	20	0.38	0.26	34.478	1.31	0.0518	2.45	277.5	6.8	184.3	2.4
7.1	363	130	13	0.36	0.37	34.271	1.37	0.0527	2.49	315.5	7.8	185.4	2.5
3.1	775	300	29	0.39	0.49	34.024	1.18	0.0537	2.01	357.2	7.2	186.7	2.2
2.2	783	330	30	0.42	0.17	33.877	1.24	0.0511	1.72	246.7	4.2	187.5	2.3
R.6308.1. Batterbee Mountains granite													
102.1x	110	62	4	0.56	0.93	37.281	2.33	0.0571	5.71	495.8	28.3	170.6	4.0
101.1x	143	80	5	0.56	0.80	36.781	2.09	0.0561	8.10	454.7	36.8	172.9	3.6
6.1x	531	376	16	0.71	0.92	36.735	1.23	0.0570	1.74	490.4	8.5	173.1	2.1
7.1x	108	59	3	0.54	3.49	36.183	1.88	0.0775	2.67	1133.1	30.3	175.7	3.3
4.1	114	59	3	0.52	3.03	35.649	2.06	0.0738	2.94	1036.3	30.5	178.3	3.7
8.1	384	355	13	0.92	0.72	35.478	1.41	0.0554	2.09	428.0	9.0	179.2	2.5
2.1	204	125	6	0.61	1.55	35.334	1.47	0.0620	2.03	673.8	13.7	179.9	2.6
1.1	195	104	6	0.54	1.56	35.128	1.91	0.0621	3.93	677.2	26.6	180.9	3.4
3.1	138	86	4	0.63	2.58	34.680	1.95	0.0702	2.27	933.9	21.2	183.3	3.6
11.1	136	78	4	0.58	2.11	34.595	1.80	0.0665	2.35	821.8	19.3	183.7	3.3
5.1	162	97	5	0.60	1.84	34.490	1.73	0.0643	3.42	751.5	25.7	184.2	3.2
2.2	447	410	16	0.92	0.69	34.280	2.91	0.0552	2.83	418.7	11.8	185.4	5.4
9.1	185	100	6	0.54	2.04	34.075	1.60	0.0659	2.61	803.2	21.0	186.5	3.0
14.1	142	84	5	0.59	1.53	33.794	1.90	0.0618	2.36	667.9	15.8	188.0	3.6
10.1	73	36	2	0.49	4.51	33.551	2.12	0.0856	4.25	1328.5	56.5	189.3	4.0
13.1	248	173	8	0.70	1.60	33.502	1.42	0.0624	1.94	689.2	13.4	189.6	2.7

12.1i	86	13	13	0.15	1.25	6.523	2.47	0.0812	3.09	1226.8	37.9	919.4	22.7
R.7170.1. Mount Sullivan granodiorite													
9.1	312	185	11	0.6	0.60	36.310	2.05	0.0546	2.99	395.5	11.8	175.1	3.6
5.1	471	116	15	0.2	0.23	35.134	1.89	0.0516	2.75	269.5	7.4	180.9	3.4
10.1	231	92	8	0.4	0.81	35.056	1.88	0.0563	3.00	462.2	13.9	181.3	3.4
8.1	109	88	4	0.8	1.07	34.994	2.55	0.0583	4.13	541.8	22.4	181.6	4.6
7.1	193	117	7	0.6	1.64	34.765	1.99	0.0628	4.63	702.1	32.5	182.8	3.6
6.1	267	96	9	0.4	0.38	34.424	2.22	0.0528	3.29	321.5	10.6	184.6	4.1
4.1	68	57	3	0.8	0.71	34.233	3.62	0.0555	5.03	430.8	21.7	185.6	6.7
2.1	505	159	17	0.3	0.28	34.125	1.40	0.0520	1.79	284.1	5.1	186.2	2.6
3.1	69	63	3	0.9	1.28	33.414	2.98	0.0600	4.60	602.1	27.7	190.1	5.7
1.1i	401	293	20	0.7	0.26	26.531	1.70	0.0532	1.82	336.5	6.1	238.5	4.1

[1]Analysis identification. Identifyers followed by x (recent Pb loss), i (inherited grain) or u (high uranium content) indicate analyses excluded from age calculations.
[2]Percentage of common ^{206}Pb estimated from the measured ^{204}Pb. Data is not corrected for common Pb, except for values given in parentheses.

Table 2: Sr-Nd isotope geochemistry

Sample	Location	Age	Sm	Nd	$^{147}Sm/^{144}Nd$	$^{143}Nd/^{144}Nd$	$^{143}Nd/^{144}Nd_i$	eps(Nd)	Rb	Sr	Rb/Sr	$^{87}Rb/^{86}Sr$	$^{87}Sr/^{86}Sr$	$^{87}Sr/^{86}Sr_i$
R.7170.1	*Mount Sullivan*	183	6.72	33.47	0.1213	0.512317	0.512171658	-4.5	356.2	109.6	3.25	9.424	0.730279	0.705758
R.2143.3	*Engel Peaks*	188	7.52	39.62	0.11478	0.51236	0.512218802	-3.5	145	43.8	3.356	9.733	0.732115	0.706097

Detailed analytical procedures are in the supplementary file. Rb-Sr and Sm-Nd isotope analyses were performed at NIGL, Keyworth, UK.